ACS APPLIED MATERIALS & INTERFACES

RESEARCH ARTICLE

www.acsami.org

Molecular Layer-by-Layer Self-Assembly and Mercury Sensing Characteristics of Novel Brush Polymers Bearing Thymine Moieties

Jungwoon Jung,[†] Jin Chul Kim,[†] Yecheol Rho,[†] Mihee Kim,[†] Wonsang Kwon,[†] Heesoo Kim,[*,‡] and Moonhor Ree[*,†]

[†]Department of Chemistry, Division of Advanced Materials Science, Center for Electro-Photo Behaviors in Advanced Molecular Systems, Polymer Research Institute, and BK School of Molecular Science, Pohang University of Science and Technology, Pohang 790-784, Republic of Korea

[‡]Department of Microbiology and Dongguk Medical Institute, Dongguk University College of Medicine, Gyeongju 780-714, Republic of Korea

Supporting Information

ABSTRACT: Two new brush polyoxyethylenes bearing thymine moieties at the bristle ends have been synthesized as model polymers in which the chemical loading of the thymine functional group into the polymer is maximized: poly(oxy(11-thyminoacetyloxyundecylthiomethyl)ethylene) (PECH(S)-T) and poly(oxy(11-thyminoacetyloxyundecylsulfonylmethyl)-ethylene) (PECH(SO_2)-T). These brush polymers are thermally stable up to around 225 °C, and their glass transitions occur in the range 23−27 °C, but they have significantly different properties despite the similarity of their chemical structures. In particular, PECH(SO_2)-T films exhibit better performance in sensing mercury ions than PECH(S)-T films. These differences were found to originate in the differences between their morphological structures. The PECH(SO_2)-T film has a multi-bilayer structure without interdigitation, in which the layers stack along the out-of-plane of the film and provide a thymine-rich surface. In contrast, the PECH(S)-T film is amorphous with a relatively low population of thymine moieties at the surface. This study demonstrated that a thymine-rich surface is required for recyclable thymine-based polymers to provide highly improved sensitivity and selectivity as well as full reversibility in the sensing of mercury ions. A thymine-rich surface can be achieved with a brush polymer bearing thymine moieties that can self-assemble into a multi-bilayer structure. Because of the thymine-rich surface, the PECH(SO_2)-T thin films even in only 6 nm thickness demonstrate the detection of mercury ions in aqueous solutions with a detection limit of 10^{-6} M.

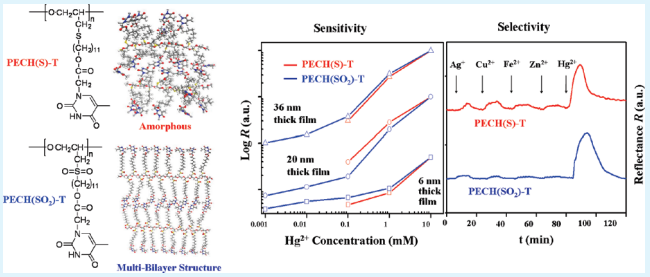

KEYWORDS: thymine containing brush polymers, thin films, self-assembly, molecular multilayer structure, hydrophilicity, water sorption, mercury ion sensing, surface plasmon resonance spectroscopy

1. INTRODUCTION

Mercury is one of the heavy metals of most concern because of its wide use in industry despite its high toxicity and its involvement in mercury-related diseases.[1] Thus, the detection of mercury ions is very important, particularly for environmental monitoring and health care; as a result, the development of functional materials that can recognize mercury ions is a research priority. Various organic materials have been reported as mercury ion sensing materials;[2−6] in these studies, spectroscopic,[2,3] electrochemical,[4] and optical techniques[5,6] were employed to characterize their mercury ion detection ability and sensitivity. Most of these organic materials have been investigated in organic media rather than aqueous media. However, due to the very high hydration of mercury ions, their direct recognition in organic solvents is more difficult than in aqueous solution. Moreover, the applications of these materials to mercury ion sensing are often limited because of interference from other metal ions. Only a few organic molecules have been found to exhibit relatively high selectivity in the detection of mercury ions in aqueous media.[3,6]

A thymine−thymine (T−T) mismatch in a DNA duplex is known to result in specific binding to a mercury ion (Hg^{2+}) and thus in the formation of a T−Hg^{2+}−T pair that is as stable as a Watson−Crick base pair.[7] Several organic molecules containing thymine moieties have been reported as probing systems for mercury ions in aqueous solutions.[8] Fluorometric and electrochemical analyses of these molecules were used to demonstrate their enhanced mercury ion selectivities and sensitivities. However, their binding reactions with mercury ions are irreversible; in other words, their binding to mercury ions is too strong. This irreversibility means that these organic systems cannot be reused;

Received: April 11, 2011
Accepted: June 8, 2011
Published: June 08, 2011

Scheme 1. Synthetic Route of the Brush Polymers Containing Thymine Moieties: Poly(oxy(11-thyminoacetyloxyundecylthiomethyl)ethylene) (PECH(S)-T) and Poly(oxy(11-thyminoacetyloxyundecylsulfonylmethyl)ethylene) (PECH(SO_2)-T)

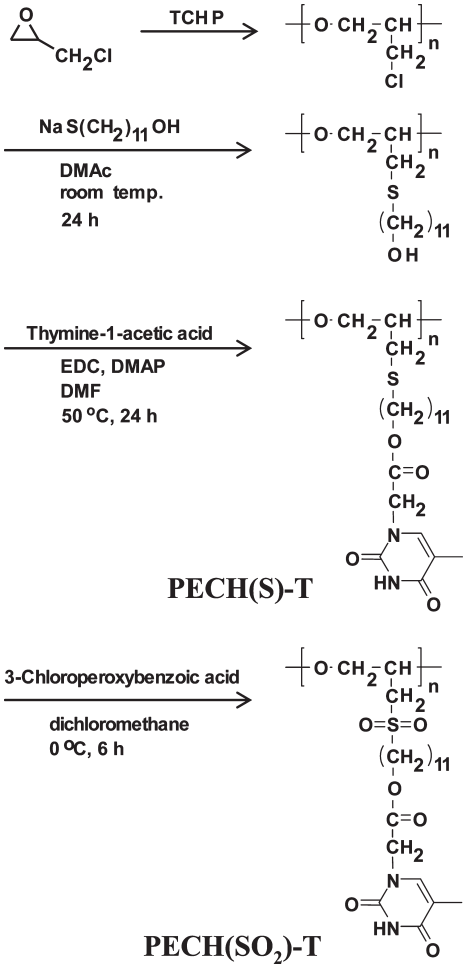

furthermore, they are not suitable for the *in situ* monitoring of mercury ions. π-Conjugate polymers bearing thymine moieties in their side groups have also been reported as mercury sensing materials with improved selectivity and reversibility.[9] However, these polymers were found to require the addition of salt solutions to fully recover to the state without mercury binding. Therefore, the development of highly sensitive and selective mercury ion sensing materials remains in the exploration stage.

In this study, we synthesized novel brush polymers bearing thymine moieties in which the chemical loading of thymine moieties is maximized and that self-assemble into molecular layer-by-layer structures (i.e., molecular lamellar structures) and provide thymine-rich surfaces: poly(oxy(11-thyminoacetyloxyundecylthiomethyl)ethylene) (PECH(S)-T) and poly(oxy(11-thyminoacetyloxyundecylsulfonylmethyl)ethylene) (PECH(SO_2)-T) (Scheme 1). These brush polymers are thermally stable up to around 225 °C. PECH(S)-T exhibits relatively high water sorption, whereas PECH(SO_2)-T exhibits low water sorption. The synchrotron grazing incidence X-ray scattering (GIXS) analysis found that thin films of PECH(S)-T are amorphous but that it forms a molecular lamellar structure in water as well as in metal ion solutions, whereas thin films of PECH(SO_2)-T always have molecular lamellar structures providing thymine-rich surfaces; this lamellar structure is retained in water and metal ion solutions. Surface plasmon resonance spectroscopy (SPRs) analysis was performed, and it was found that PECH(SO_2)-T exhibits excellent sensitivity, selectivity, and reversibility in sensing mercury ions in aqueous solutions, with properties that are superior to those of PECH(S)-T. We propose a strategy based on the control of morphological nanostructure for developing high performance polymers for the chemical monitoring of metal ions.

2. EXPERIMENTAL SECTION

2.1. Materials. All chemicals were purchased from Aldrich Chemical Company and used as received. For the preparation of metal ion solutions, mercury(II) chloride, copper(II) chloride, zinc(II) chloride, iron(II) chloride tetrahydrate, and silver(I) nitrate were dissolved in deionized water.

2.2. Polymer Synthesis. PECH(S)-T, a brush polymer containing the thymine moiety at the bristle end, was synthesized in a three step reaction. In the first step, poly(epichlorohydrin) (PECH) was synthesized from epichlorohydrin as follows. Epichlorohydrin (40 mL, 512 mmol) was cooled to −5 °C under nitrogen atmosphere. Triphenylcarbenium hexafluorophosphate (TCHP) (0.10 g, 0.26 mmol) (which is an initiator) was dissolved in dichloromethane (CH_2Cl_2) and slowly added to epichlorohydrin. The reaction solution was stirred at room temperature for 2 days. The crude polymer in CH_2Cl_2 was purified by precipitating into methanol several times and finally dried in vacuum condition at 40 °C for 12 h, giving a colorless viscous liquid. Yield = 65%. The obtained PECH product was characterized by proton and carbon nuclear magnetic resonance (^{1}H and ^{13}C NMR) spectroscopy using a 300 MHz NMR spectrometer (model DPX 300, Bruker, Germany) and Fourier transform infrared (FTIR) spectroscopy using an infrared (IR) spectrometer (model Research Series, ATI Mattson, USA). ^{1}H NMR (300 MHz, $CDCl_3$, δ (ppm)): 3.89−3.49 (br, 5H, OCH, OCH_2, CH_2Cl). ^{13}C NMR (75 MHz, $CDCl_3$, δ (ppm)): 79.70, 70.32, 44.31. IR (in film, ν (cm^{-1})): 2960, 2915, 2873, 1427, 1348, 1299, 1263, 1132, 750, 707.

In the second step, PECH was converted to poly[oxy(11-hydroxyundecanyl-thiomethyl)ethylene] (PECH−OH). PECH (3.38 g, 36.50 mmol) and sodium 11-hydroxyundecylthiolate (9.07 g, 39.70 mmol) were dissolved in 40 mL of dimethylacetamide (DMAc) and stirred at room temperature for 24 h. Then, the reaction solution was poured into 100 mL of chloroform ($CHCl_3$), and the used DMAc was eliminated by washing with deionized water several times. The solution was dried over anhydrous magnesium sulfate and filtered off. The filtrate was concentrated under reduced pressure. The obtained polymer product was poured into cold *n*-hexane, and then the polymer product in white powder was filtered, followed by drying in vacuum. Yield = 84%. ^{1}H NMR (300 MHz, $CDCl_3$, δ (ppm)): 3.70−3.59 (br, 3H, OCH, OCH_2), 2.75−2.52 (m, 4H, SCH_2), 1.57−1.13 (m, 18H, CH_2). ^{13}C NMR (75 MHz, $CDCl_3$, δ (ppm)): 79.36−78.72, 63.07, 39.23, 33.26, 32.82, 29.75−28.53, 25.76; IR (KBr, ν (cm^{-1})): 3590-3100, 2960, 2854, 1460, 1110, 732.

In the final step, the obtained PECH−OH was again converted to the target polymer PECH(S)-T. PECH−OH (0.26 g, 1.00 mmol OH), thyminoacetic acid (0.20 g, 1.10 mmol), *N*-(3-dimethylaminopropyl)-*N*′-ethylcarbodiimide hydrogenchloride (EDC, 0.47 g, 3.00 mmol), and 4-(dimethylamino)pyridine (DMAP, 0.18 g, 1.50 mmol) were dissolved in 20 mL of dimethylformamide (DMF) and stirred at 45 °C for 24 h. The reaction solution was precipitated in diethyl ether and filtered. The filterate was purified by column chromatography (20 % methanol/CH_2Cl_2, R_f = 0.8). The obtained product was dried, giving the target product as a white powder. Yield = 50%. ^{1}H NMR (300 MHz,

dimethylsulfoxide-d_6 (DMSO-d_6), δ(ppm)): 11.4 (s, 1H, NH), 7.47 (s, 1H, Ar−H), 4.45 (s, 2H, CH_2), 4.05 (s, 2H, CH_2), 3.70−3.59 (br, 3H, OCH, OCH_2), 2.75−2.52 (m, 4H, CH_2SCH_2), 1.74 (s, 3H, Ar−CH_3), 1.57−1.13 (m, 18H, CH_2). ^{13}C NMR (75 MHz, DMSO-d_6, δ (ppm)): 69.3, 165.4, 152.8, 142.6, 109.7, 79.36−78.72, 69.42, 66.14, 49.5, 39.23, 33.44, 32.82, 29.75−28.53, 25.76, 13.04. IR (KBr, ν (cm^{-1})): 3590-3100, 2960, 2854, 1707, 1664, 1632, 1460, 1419, 1200, 1110, 830, 732.

Some portion of the PECH(S)-T product was further converted to PECH(SO_2)-T. PECH(S)-T (0.32 g, 1.00 mmol S) was dissolved in CH_2Cl_2 and stirred at 0 °C for 10 min. Then, 3-choroperoxybenzoic acid (0.17 g, 1.00 mmol) was added and stirred for 6 h. After the reaction was completed, the solvent was evaporated and washed with methanol and ether several times, followed by drying at room temperature in vacuum. The target product was obtained as a white powder. Yield = 100%. ^{1}H NMR (300 MHz, DMSO-d_6, δ (ppm)): 11.4 (s, 1H, NH), 7.47 (s, 1H, Ar−H), 4.45 (s, 2H, CH_2), 4.05 (s, 2H, CH_2), 3.70−3.59 (br, 3H, OCH, OCH_2), 3.48−2.94 (m, 4H, $CH_2SO_2CH_2$), 1.74 (s, 3H, Ar−CH_3), 1.57−1.13 (m, 18H, CH_2). ^{13}C NMR (75 MHz, DMSO-d_6, δ (ppm)): 169.3, 165.4, 152.8, 142.6, 109.7, 79.36−78.72, 69.42, 66.14, 49.5, 52.1, 51.3, 32.82, 29.75-28.53, 25.76, 13.04. IR (KBr, ν (cm^{-1})): 3590−3100, 2960, 2854, 1707, 1664, 1632, 1460, 1419, 1320, 1200, 1157, 1145, 1320, 1110, 830, 732.

2.3. Polymer Film Preparation. For each brush polymer, solutions of various concentrations (0.1−1.0 wt %) were prepared in chloroform and filtered using disposable syringes equipped with a polytetrafluoroethylene filter of pore size 0.2 μm. The filtered solutions were deposited on various substrates (silicon wafers, glass slides, and gold-coated glass prisms (BaK4, barium crown glass)) by a spin-coating process and then dried at 60 °C for 1 day under vacuum. Thicknesses of the obtained films were determined to range 20−100 nm by ellipsometry (model M-2000, Woollam, Lincoln, NE, USA) and α-stepper (Veeco Company, CA, USA). For GIXS analysis, some of the films were further immersed in various metal ion solutions of 1 mM for 6 h, and then the metal ion solutions on the film surface were removed by nitrogen blowing.

2.4. Measurements. Thermal properties were measured by differential scanning calorimetry (DSC) (model DSC-220CU, Seiko Instruments, Japan) and thermogravimetry (TGA) (model TG/DTA-6300, Seiko, Japan). During the measurements, dry nitrogen gas was used for purging with a flow rate of 80 mL/min, and a ramping rate of 10.0 °C/min was employed. Molecular weight of the synthesized PECH polymer was determined using a gel permeation chromatograph (GPC; Polymer labs, model PL-GPC 210) equipped with a set of gel columns (2 columns of PL Gel Mixed-C). The system was equilibrated at 25 °C in anhydrous tetrahydrofuran (THF), which was used as the polymer solvent and eluent with a flow rate of 0.8 mL/min, and calibrated with polystyrene standards (1,330−1,090,000 $\overline{M}_w$; $\overline{M}^w$ is the weight-average molecular weight).

GIXS measurements using an X-ray radiation source (λ = 0.138 nm) were carried out at the 4C1 and 4C2 beamlines of the Pohang Accelerator Laboratory (PAL) at Pohang University of Science & Technology.[10,11] A sample-to-detector distance of 132 mm was used. Samples were mounted on a homemade z-axis goniometer equipped with a vacuum chamber at room temperature. The incident angle α_i of the X-ray beam was set at 0.16°, which is between the critical angles of the polymer films and the silicon substrates ($\alpha_{c,f}$ and $\alpha_{c,s}$). Scattering angles were corrected according to the positions of the X-ray beams reflected from the silicon substrate interface with changing incidence angle α_i and with respect to a pre-calibrated silver behenate (TCI, Japan) powder. Aluminum foil pieces were employed as semi-transparent beam stops because the intensity of the specular reflection from the substrate is much stronger than the intensity of GIXS near the critical angle. Each measurement was collected for 30 s using a two-dimensional (2D) charge-coupled detector (CCD: Roper Scientific, Trenton, NJ, USA).

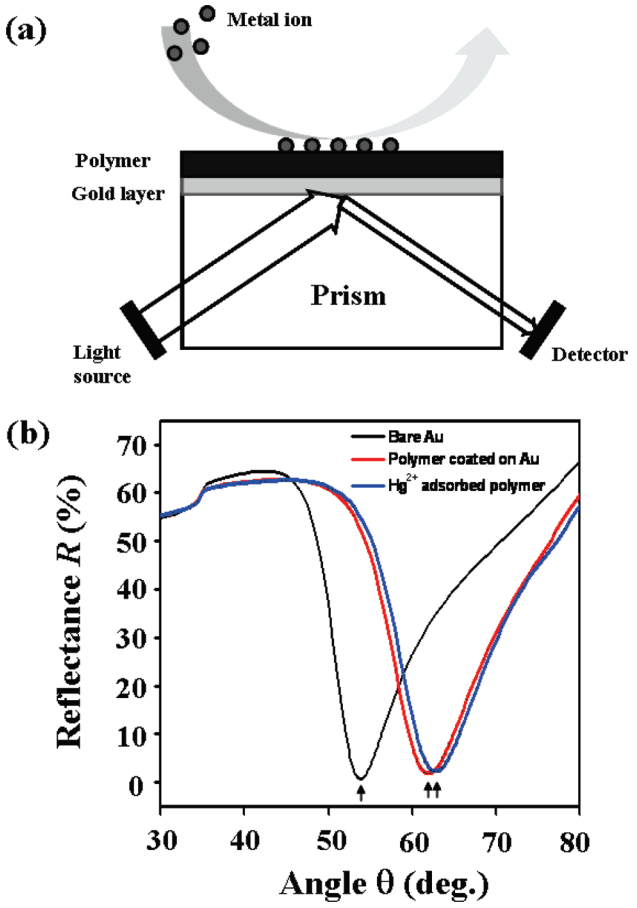

Figure 1. (a) Schematic diagram of SPRs. (b) Reflectance R profiles measured by SPRs as a function of the incidence angle of the light source: bare Au surface (black), the surface coated with a brush polymer, PECH(S)-T (red), and the brush polymer coated surface with Hg^{2+} adsorption (blue). Each profile reveals the minimum at a SPR angle. For the Hg^{2+} adsorption, an aqueous solution of 1.0 mM was used.

Water contact angles were measured at 25 °C using a contact angle meter (KSV instruments, Japan). The water contact angle measurements were performed at an interval of 10 s for 90 s. Thickness variations by swelling properties were measured by a spectroscopic ellipsometry (model M-2000, Woollam, Lincoln, NE, USA) with a liquid cell. The angle of incidence light was controlled to be 75°, and the window angle of the liquid cell was set to be 75° so as to be perpendicular to incidence light. The thickness variation measurements were carried out every 10 min.

SPRs measurements were carried out by using a SPR spectrometer (K-MAC, Daejeon, Korea) equipped with a semiconductor laser (633 nm) (Figure 1a), according to a method described elsewhere.[12] For the measurements, each brush polymer was spin-coated with a thickness of 15−20 nm onto glass prisms deposited with a 50 nm thick gold layer. The prisms were mounted on a rotating plate to control the angle of incident light, and then liquid fluids containing metal ions were applied to the surface of the polymer thin films. The polymer thin film on the gold surface was identified by the SPR angle shift, and Hg^{2+} adsorption could be detected in the same manner (Figure 1b). Quantitative analysis was investigated with reflectance change. The Hg^{2+} solutions with concentration ranging from 0.001 to 10 mM were prepared for the quantitative analysis. Each concentration of Hg^{2+} solution was injected for 10 min, and then the sample solution was replaced by deionized water for 10 min. In the same manner, the

selectivity of each brush polymer film for metal ions such as Hg^{2+}, Zn^{2+}, Cu^{2+}, Fe^{2+}, and Ag^{+} was investigated. In this selectivity study, the concentration of each metal ion was fixed at 0.1 mM. To determine the relationship between film thickness and sensing ability, the thickness of brush polymer films was varied over the range of 6−36 nm.

3. RESULTS AND DISCUSSION

3.1. Polymer Synthesis and Thermal Properties. PECH(S)-T, a poly(epichlorohydrin)-based brush polymer containing thymine moieties was prepared in a three-step reaction (Scheme 1). In the first step, PECH was synthesized via a cationic ring-opening polymerization initiated by using TCHP as an initiator according to a method previously reported in the lierature.[13] Its number-average molecular weight ($\overline{Mn}$) and polydispersity index (PDI) were determined to be 22700 mol/g and 1.68, respectively, by GPC analysis against polystyrene standards. In the second step, PECH−OH was obtained by reacting PECH and sodium salt of 11-mercapto-1-undecanol in DMAc. The obtained PECH−OH was characterized by ^{1}H and ^{13}C NMR spectroscopy. The NMR spectroscopy analysis confirms that the bristle was incorporated with 100% yield into the PECH polymer (see the data in the Experimental Section). Therefore, the yield of the S_N2 type reaction between PECH and sodium alkyl thiolate was quantitative. To synthesize the sulfur-linked PECH brush polymer containing the thymine moiety (PECH(S)-T), a conventional esterification was performed for the PECH−OH polymer by using EDC and DMAP in DMF. After the reaction was completed, the reaction mixture was purified using silica gel column chromatography. A representative ^{1}H NMR spectrum of the synthesized polymer is presented in Figure S1 (Supporting Information). The degree of conversion was monitored by using the signal integration ratio corresponding to the ester ($CH_2C(=O)O$) group at 4.05 ppm and the alkyl side chain group at 1.67−1.05 ppm. Peaks characteristic of thymine moieties were also found at 11.4, 7.47, 4.45, and 1.74 ppm. These analysis results confirm that the incorporation of the thymine moiety to the bristle end proceeded with 100% yield. To further convert some of the sulfur-linked brush polymer to the sulfone-linked brush polymer (PECH(SO_2)-T), oxidation was successfully performed by using 3-chloroperoxybenzoic acid at 0 °C as previously reported.[14]

Thermal stabilities and phase transitions of the brush polymers were investigated in a nitrogen atmosphere. The TGA analysis found that the brush polymers exhibit almost the same degradation temperature, around 225 °C (Figure S2a in Supporting Information). PECH(SO_2)-T contains SO_2 and therefore undergoes more mass loss than PECH(S)-T. For both of the polymers, degradation of the alkyl linkers occurs before degradation of the backbone.

The DSC analysis found that the brush polymers reveal only glass transition (Figure S2b in Supporting Information); the glass transition temperatures (T_g) of PECH(S)-T and PECH(SO_2)-T are 23 °C and 27 °C, respectively. The difference between these temperatures is mainly due to the difference in the side chain flexibilities of the two polymers, which originates in their different side chain linkers.

3.2. Thin Film Structures. GIXS measurements were performed on brush polymer thin films with a thickness of 50 nm in order to determine their structures and identify structural changes upon binding with water and metal ions. The GIXS scattering data are displayed in Figures 2 and 3.

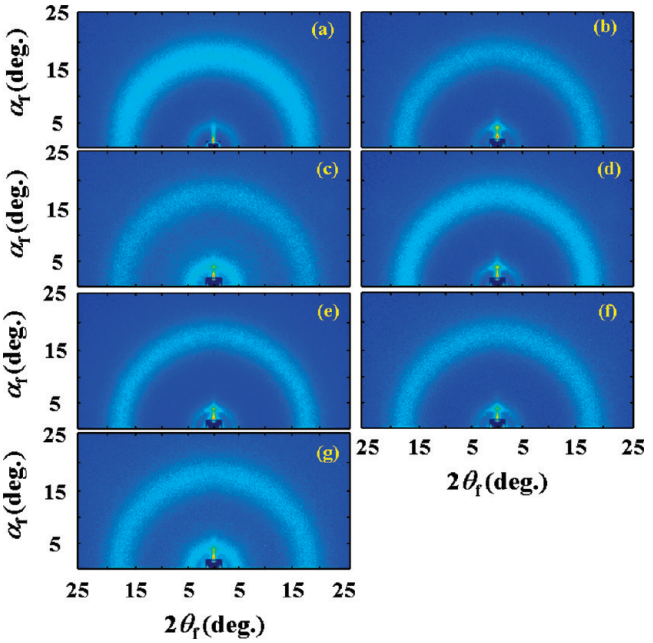

Figure 2. 2D GIXS patterns of PECH(S)-T in thin films in (a) dry condition and treated with (b) water, (c) Hg^{2+}, (d) Zn^{2+}, (e) Cu^{2+}, (f) Fe^{2+}, and (g) Ag^{+} ion solution at room temperature. The measurements were carried out with $\alpha_i = 0.16°$ in vacuum.

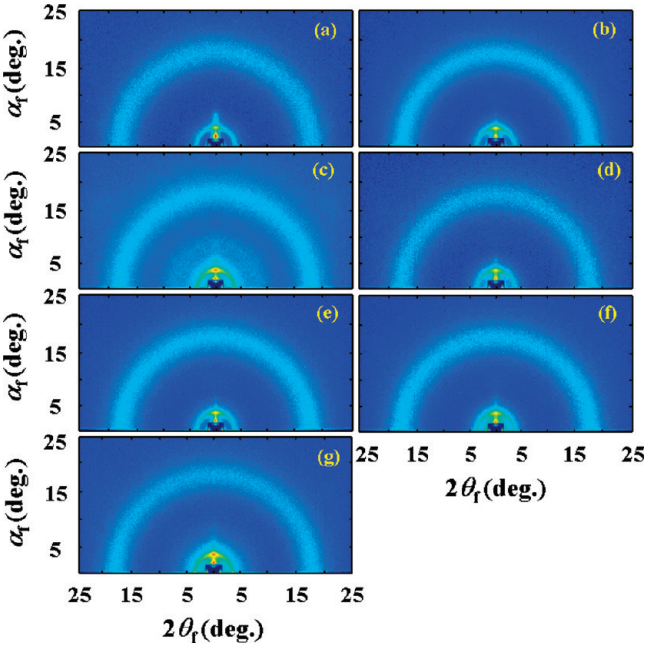

Figure 3. 2D GIXS patterns of PECH(SO_2)-T in thin films in (a) dry condition and treated with (b) water, (c) Hg^{2+}, (d) Zn^{2+}, (e) Cu^{2+}, (f) Fe^{2+}, and (g) Ag^{+} ion solution at room temperature. The measurements were carried out with $\alpha_i = 0.16°$ in vacuum.

Figure 2 shows the GIXS patterns of PECH(S)-T thin films under dry conditions and after treatment with water and various metal solutions. From these GIXS patterns, the out-of-plane scattering profiles were extracted along the α_f direction at $2\theta_f = 0.00°$, and the scattering profiles were azimuthally extracted along the angle of the scattering peak maximum in the low angle

Table 1. Structural Parameters of the Brush Polymers in Thin Films, Which Were Determined by GIXS Measurements and Data Analysis

		scattering spot in low angle region[a]				ring scatterings			
						1st ring		2nd ring	
polymer in thin film	treated solution	angle [b] (deg)	*d*-spacing (nm)	FWHM [c] (deg)	L[d]	angle [e] (deg)	*d*-spacing (nm)	angle [e] (deg.)	*d*-spacing (nm)
PECH(S)-T	(dry) [f]					4.58	1.73	16.87	0.47
	water	3.92	2.02	9.1	4.04	4.07	1.94	17.40	0.46
	Hg^{2+}	3.79	2.09	10.7	4.18	4.32	1.83	17.66	0.45
	Zn^{2+}	3.79	2.09	9.6	4.18	3.81	2.08	17.32	0.46
	Cu^{2+}	3.88	2.04	9.7	4.08	3.88	2.04	17.40	0.46
	Fe^{2+}	3.80	2.08	10.2	4.16	3.80	2.08	17.44	0.46
	Ag^{+}	3.80	2.08	10.4	4.16	4.30	1.84	17.40	0.46
PECH(SO_2)-T	(dry) [f]	3.96	2.00	15.1	4.00			17.54	0.45
	water	3.79	2.09	17.1	4.18			17.20	0.46
	Hg^{2+}	3.67	2.16	13.1	4.32			17.54	0.45
	Zn^{2+}	3.79	2.09	15.3	4.18			17.26	0.46
	Cu^{2+}	3.73	2.12	16.9	4.24			17.26	0.46
	Fe^{2+}	3.76	2.10	14.4	4.20			17.26	0.46
	Ag^{+}	3.69	2.14	13.2	4.28			17.26	0.46

[a] The scattering spot appeared along the α_f direction at $2\theta_f = 0°$ (Figures 2 and 3). [b] The out-of-plane exit angle α_f. [c] The full-width-at-half maximum (FWHM) determined from the azimuthal angle profile of the scattering spot in the low angle region, which was extracted from the measured 2D GIXD pattern. [d] The mean layer thickness estimated from the second order scattering spot. [e] The in-plane exit angle $2\theta_f$. [f] The polymer film in dry condition.

region. Furthermore, the in-plane scattering profiles were extracted along the $2\theta_f$ direction at $\alpha_f = 0.00°$. The resulting scattering profiles are presented in Figure S3 (Supporting Information). As can be seen in Figures 2a and S3 (Supporting Information), at room temperature the dry films (i.e., the untreated films) of PECH(S)-T produce featureless scattering patterns with only two isotropic halo rings. The first halo peak at $2\theta_f = 4.58°$ corresponds to a *d*-spacing of 1.73 nm, and the second halo peak at $2\theta_f = 16.87°$ corresponds to a *d*-spacing of 0.47 nm (Table 1). Given the T_g and the chemical structure, the first scattering ring was identified as an amorphous halo originating from the mean inter-chain distance of the brush polymer molecules, and the second scattering ring was identified as another amorphous halo attributed to the mean interdistance between the bristles in the polymer chains.

Surprisingly, the polymer films treated with water and aqueous metal ion solutions produce a new scattering spot rather than an isotropic scattering ring in the low angle region, which is quite different from the results for the dry film (Figures 2 and S3 (Supporting Information)). The scattering spot appears along the meridian line at $2\theta_f = 0.00°$; further, the scattering spot is shifted slightly towards the low angle region with respect to the first amorphous halo ring of the dry film. The *d*-spacing varies in the range 2.02 to 2.09 nm depending on film treatment (Table 1). These *d*-spacing values are larger than the mean inter-chain distance (1.73 nm) of the dry film. These results collectively indicate that a layer-by-layer structure (i.e., a lamellar structure) is formed in the films in which the layers are stacked along the out-of-plane of the film. Further, the film treatments with water and metal ion solutions induce the brush polymer molecules to form a lamellar structure. These results are a clue that the metal ions and water molecules favorably bind to the thymine moieties in the polymer. However, for the films, a very weak ring scattering is still present around the scattering spot (Figures 2b−g); its *d*-spacing is slightly smaller than or close to that of the scattering spot (Table 1). The presence of this weak ring scattering indicates that there is a small fraction of amorphous phase and/or small regions with randomly oriented lamellar structure in the films. Moreover, no higher order peaks of the scattering spot were observed for all of the films, which indicates that the lamellar structures have no long-range order and low perfectness. From these results and considering the brush polymer's chemical structure, the scattering spot can be assigned as the second order diffraction of the lamellar structure (i.e., a molecular multi-bilayer structure) formed in the films. The layer thickness L (i.e., the long period) of the molecular multi-bilayer structure was found to be in the range 4.04 to 4.18 nm, depending on film treatment (Table 1).

The determined layer thicknesses are close to twice the length (2.05 nm) of a fully extended bristle without a thymine moiety but smaller than twice the length (2.51 nm) of a fully extended bristle with a thymine moiety; the length of the fully extended bristles was estimated by using a molecular simulation performed with the Cerius^2 software package (Accelrys, San Diego, CA, USA). Thus, it is likely that the bristles in the multi-bilayer structure are partially interdigitated between the adjacent molecular layers. However, the ring scattering at $2\theta_f = 17.32°$ to 17.66° (which is attributed to the mean interdistance of the bristles in the films) is isotropic for all of the films and therefore is similar to the second amorphous halo ring observed for the dry film (Figures 2 and S3 (Supporting Information)). For the isotropic scattering ring, the *d*-spacing was determined to be in the range 0.45−0.46 nm, i.e., the variation with treatment is slight (Table 1); these *d*-spacing values are slightly smaller than that of the second amorphous halo ring for the dry film. These results indicate that the bristles in the brush polymer films treated with

water and metal ions are laterally closer than those in the dry film. These results also show that the bristles are not fully extended, which reduces the layer thickness. Furthermore, the layer thickness L in the multi-bilayer structure varies as a result of the water and metal ion solution treatments; in other words, the layer thickness change depends on the nature (i.e., the size and binding scheme) of the molecular and ionic sources bound to the thymine moieties (Table 1). These results suggest that the binding of water molecules and metal ions to the thymine moieties takes place favorably in the interlayers of the multi-bilayer structure. In conclusion, the likelihood of interdigitation between the adjacent molecular layers in the multi-bilayer structure is very low.

Figure 3 shows the scattering patterns of the PECH(SO_2)-T thin films under dry conditions and after treatment with water and metal solutions. From these GIXS patterns, the out-of-plane and in-plane scattering profiles as well as the azimuthal angle profiles were extracted as for the PECH(S)-T films. The extracted scattering profiles are presented in Figure S4 (Supporting Information). The scattering data analysis results are summarized in Table 1.

As shown in Figure 3a, dry PECH(SO_2)-T produces a scattering pattern that is similar to those of the PECH(S)-T films treated with water and metal ion solutions. Thus, even in the dry PECH(SO_2)-T film the brush polymer molecules form a multi-bilayer structure with layers stacked along the out-of-plane of the film. However, the dry film produces two scattering spots rather than a single spot along the meridian line. These spots correspond to d-spacings of 2.00 and 1.33 nm, respectively; the d-spacing for the second spot is two thirds of that for the first one. These results indicate that the two scattering spots are the second and third reflections of the multi-bilayer structure. Thus, we estimate from the scattering spots that the thickness of the layers in the multi-bilayer structure is 4.00 nm. We conclude that the multi-bilayer structure in the dry film has better ordering along the direction of the layer stacks than those formed in the PECH(S)-T films treated with water and metal ion solutions.

The scattering spot at $\alpha_f = 3.96°$ is now discussed further. This scattering spot has a tail-like ring (Figure 3a). This ring tail is quite sharp, which suggests that there are small regions of the multi-bilayer structure that are randomly oriented in the film. However, the isotropic ring scattering at $2\theta_f = 17.54°$ has a d-spacing of 0.45 nm, which is almost the same as that of the PECH(S)-T film treated with water. This scattering ring is attributed to the mean interdistance of the bristles in the polymer film, which indicates that in the multi-bilayer structure the bristles are laterally packed in an irregular manner. This scattering characteristic also shows that the bristles are not fully extended. These morphological and chemical structure characteristics indicate that there is not likely to be interdigitation between the adjacent molecular layers in the multi-bilayer structure of the film.

PECH(S)-T and PECH(SO_2)-T are composed of the same backbone, and their bristle lengths are the same (Scheme 1). However, the dry films of these polymers have quite different morphological structures (featureless versus a multi-bilayer structure), as discussed above. Thus, the question arises as to the reason for the different morphological structures of their films. The PECH polymer was found to be amorphous. Each bristle in PECH(S)-T is composed of a thymine end group and sulfur and alkyl linkers. The thymine end group has hydrogen bonding sites that make some contribution to structure formation. In contrast, the sulfur and alkyl linkers are very flexible

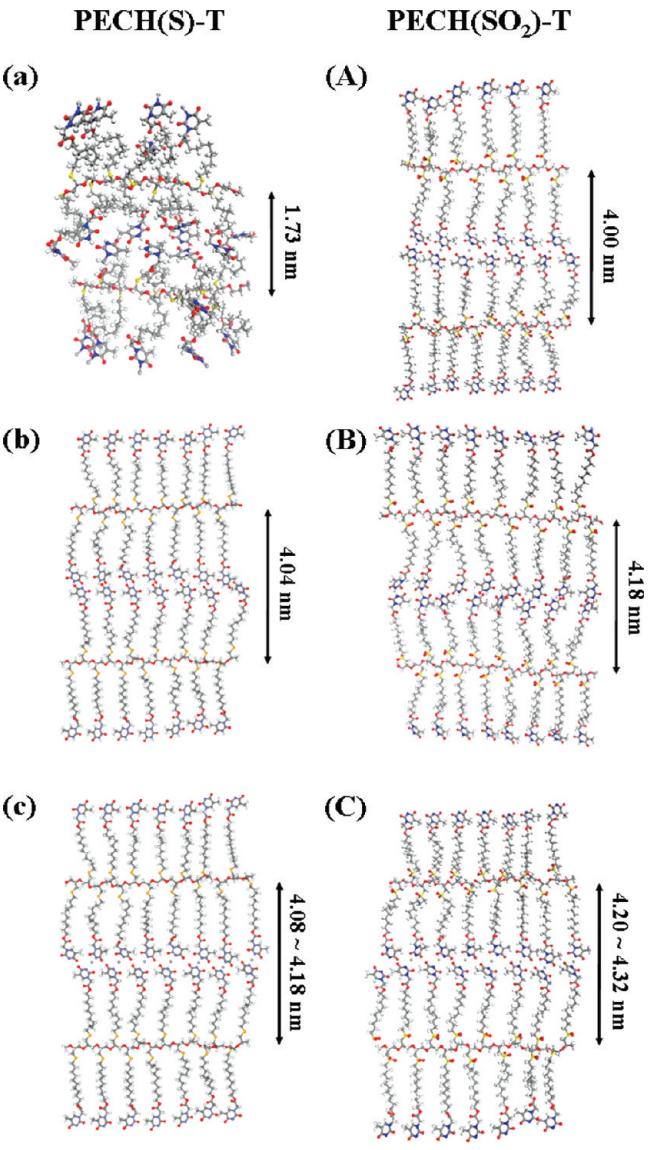

Figure 4. Proposed structural models of the brush polymers in thin films in (a, A) dry condition and treated with (b, B) water and (c, C) metal ion solutions. The metal solutions were Hg^{2+}, Zn^{2+}, Cu^{2+}, Fe^{2+}, and Ag^{+} ions.

and thus make no significant contribution to structure formation. Taking these characteristics into account, we attribute the absence of structure formation in the dry PECH(S)-T film to the contributions of the flexible backbone and bristle linkers, which override the hydrogen bonding of the thymine moieties. In contrast, the bristles of PECH(SO_2)-T contain sulfone rather than sulfur linkers. The sulfone linker has two local dipole moments along the two sulfur−carbon bonds. Thus, dipole−dipole interactions occur between the individual bristles via the sulfone sites and thus contribute to structure formation. Thus, the multi-bilayer structure of the dry PECH(SO_2)-T film is attributed to the contributions of the sulfone linkers and thymine end groups, which override those of the flexible backbone and the alkyl linkers. Because of the favorable formation of multi-bilayer structures, PECH(SO_2)-T films provide thymine-rich surfaces.

The PECH(SO_2)-T films treated with water and metal ion solutions produce scattering patterns that are similar to that of

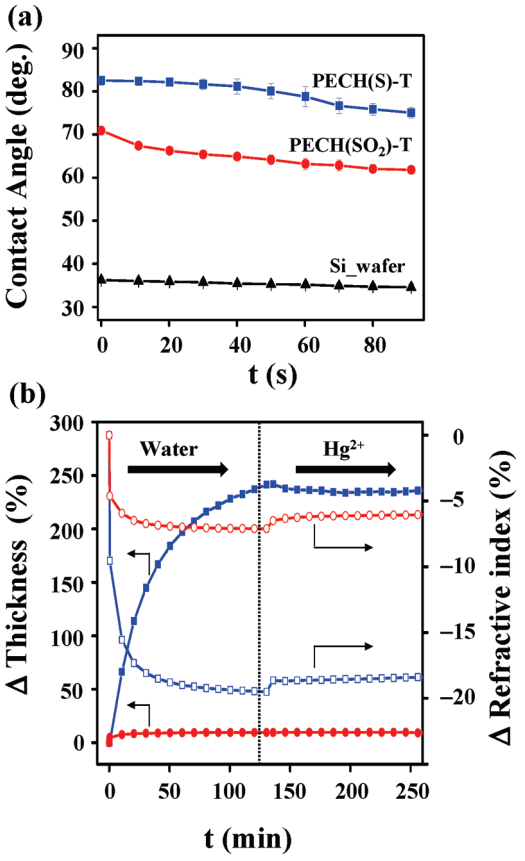

Figure 5. (a) Water contact angle variations of the polymer films at room temperature: PECH(S)-T (filled squares), PECH(SO_2)-T (filled circles), and silicon wafer (filled triangles). (b) Variations in the thicknesses and refractive indices of the brush polymer films immersed in water and Hg^{2+} solution, measured at room temperature with ellipsometry: PECH(S)-T (squares) and PECH(SO_2)-T (circles). The filled symbols are the thickness results, and the open symbols are the refractive index results; the thickness and refractive index variations were normalized to those of the film in dry condition, respectively. Films with a thickness of 20 nm were used.

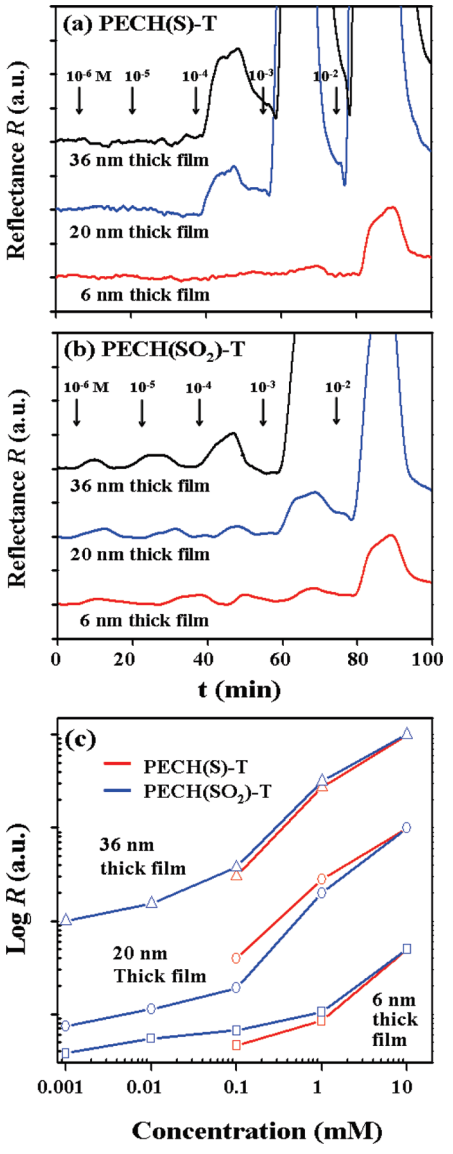

Figure 6. Reflectance variations of the brush polymer films with various thicknesses, as measured by varying the concentration of Hg^{2+} ions: (a) PECH(S)-T and (b) PECH(SO_2)-T. The changes in the reflectances of the brush polymer films in panels a and b are compared in panel c. For each film, measurements were carried out at a fixed angle at which the film in dry condition revealed the minimum light reflectance. In these measurements, each solution with a specific concentration of Hg^{2+} was injected for 10 min, and then the sample solution was replaced by deionized water for 10 min.

the dry film (Figures 3 and S4 (Supporting Information)). These results indicate that overall the multi-bilayer structure formed in the film is retained during the treatments with water and aqueous metal ion solutions. In particular, the irregular lateral packing of the bristles in the films is unchanged by treatment with water or metal ion solution (Table 1). However, the layer thickness L in the multi-bilayer structure can increase, depending on the treatment (Table 1). These results again indicate that there is no interdigitation between the adjacent layers in the multi-bilayer structure.

In the light of the above GIXS analysis results, we propose molecular multi-bilayer structure models of the thin films of the brush polymers bearing thymine moieties on the bristle ends before and after treatment with water and metal ion solutions. The proposed structural models are presented in Figure 4.

3.3. Mercury Sensing Characteristics. The water contact angle measurements were conducted at room temperature. In these measurements, a precleaned silicon wafer was used as the control. As can be seen in Figure 5a, PECH(SO_2)-T has a lower contact angle than PECH(S)-T, which indicates that PECH-(SO_2)-T has a more hydrophilic surface than PECH(S)-T. During the contact of the PECH(SO_2)-T and PECH(S)-T films with water, the contact angles decrease with time. However, the contact angle decrease of PECH(SO_2)-T is smaller than that of PECH(S)-T; in other words, the change in the hydrophilicity of PECH(SO_2)-T due to water sorption is smaller. This conclusion was confirmed by examining the changes in film thickness due to water sorption, as discussed below.

The water sorption behaviors of the polymers in deionized water and Hg^{2+} solutions (1 mM) were examined by using ellipsometry. The film thickness variation was monitored for 2 h in a liquid cell filled with water, and then the ambient liquid was changed to Hg^{2+} solution. Both the films of the polymers exhibit

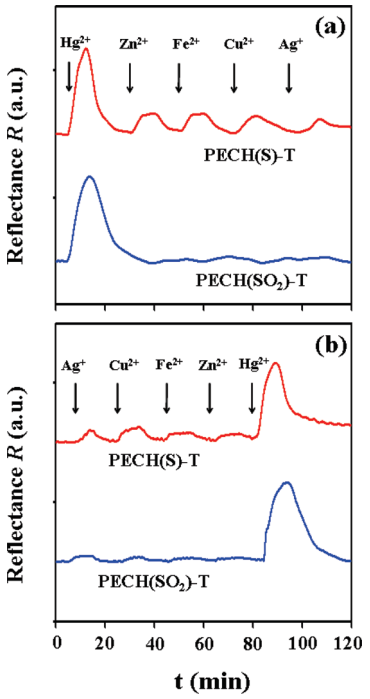

Figure 7. Reflectances of 20 nm thick polymer films measured upon the injection of a series of metal ion solutions in the following order: (a) Hg^{2+}, Zn^{2+}, Fe^{2+}, Cu^{2+}, Ag^{+}; (b) Ag^{+}, Cu^{2+}, Fe^{2+}, Zn^{2+}, Hg^{2+}. For each film, measurements were carried out at a fixed angle at which the film in dry condition revealed the minimum light reflectance. In these measurements, each metal ion solution was injected for 10 min, and then the sample solution was replaced by deionized water for 10 min. The concentration of each metal ion was 0.1 mM.

water swelling behavior. As can be seen in Figure 5b, the PECH(SO_2)-T film thickness rapidly increases for 5−10 min and then increases slowly, whereas the PECH(S)-T film thickness increases continuously, ultimately becoming much greater than that of PECH(SO_2)-T. The refractive index values of the polymer films decrease upon water sorption because the refractive index of water is lower than those of the films.

In contrast, when the Hg^{2+} solution was injected, the PECH(S)-T film thickness decreases slightly, and the refractive index also increases (Figure 5b). In the case of the PECH(SO_2)-T polymer, the film thickness is apparently unchanged but the refractive index increases, as observed for the PECH(S)-T film (Figure 5b). These results confirm that the binding of Hg^{2+} ions to the brush polymer molecules takes place where the films are in contact with the Hg^{2+} solution, which results in changes in thickness in particular in the PECH(S)-T film and in changes in the refractive indexes of the films of the polymers.

The mercury sensing behaviors of the brush polymers were further investigated for the concentration range 10^{-6} to 10^{-2} M by using SPRs. As can be seen in Figures 6a and c, PECH(S)-T films with a thickness of 6−36 nm clearly undergo reflectance changes in response to exposure to concentrations of Hg^{2+} ions of 10^{-4} M and higher. However, no reflectance changes are apparent for concentrations of Hg^{2+} ions $<10^{-4}$ M. The detection limit of PECH(S)-T for Hg^{2+} ions is thus 10^{-4} M. In contrast, PECH(SO_2)-T films clearly undergo reflectance changes in response to concentrations of Hg^{2+} ions down to 10^{-6} M (Figures 6b and c). Even in the case of very thin films (only 6 nm thick, which is close to a monolayer), the reflectance is very sensitive to changes in the Hg^{2+} ion concentration for concentrations down to 10^{-6} M. These results indicate that PECH(SO_2)-T films are highly sensitive to Hg^{2+} ions; the detection limit for Hg^{2+} ions of PECH(SO_2)-T is 10^{-6} M, which is much better than that of PECH(S)-T. Moreover, for the PECH(SO_2)-T films, the reflectance rapidly returns to its initial level upon water loading after the changes caused by Hg^{2+} ion loading, regardless of the film thickness (Figure 6b). This result shows that the binding and releasing reactions of Hg^{2+} ions in the PECH(SO_2)-T films are fully reversible. This reversibility is better than that of PECH(S)-T (Figure 6a).

We also examined the selectivities of the brush polymers for Hg^{2+} ion from other metal ions using SPRs. For each brush polymer film, reflectance changes were measured at a fixed value at which its dry film showed a minimum value in reflectance by the injection of a series of metal ion solutions in the following orders: (i) Hg^{2+}, Zn^{2+}, Fe^{2+}, Cu^{2+}, Ag^{+}; (ii) Ag^{+}, Cu^{2+}, Fe^{2+}, Zn^{2+}, Hg^{2+}. In this study, the concentration of each metal ion solution was 0.1 mM. The results are presented in Figure 7. For the PECH(S)-T films, the reflectance reveals significant increase for Hg^{2+} but relatively small increases for the other metal ions, regardless of the injection orders of the metal ion solutions. These results indicate that PECH(S)-T owns a good selectivity for Hg^{2+} ion from other metal ions. However, PECH(S)-T still exhibits certain degrees of sensing ability for the other metal ions, which were considered here. Overall, the selectivity of PECH(S)-T is in the decreasing order $Hg^{2+} \gg Fe^{2+} \approx Zn^{2+} > Cu^{2+} > Ag^{+}$. The PECH($SO_2$)-T film also exhibits significant increase in the reflectance for Hg^{2+} as observed for the PECH(S)-T film. However, the PECH(SO_2)-T film reveals almost negligible response in the reflectance for the other metal ions, regardless of the injection orders of the metal ion solutions, which is quite different from that of the PECH(S)-T film (Figure 7). The results inform us that the selectivity of PECH(SO_2)-T is in the decreasing order $Hg^{2+} \gg Fe^{2+} \approx Zn^{2+} \approx Cu^{2+} \approx Ag^{+}$. Collectively, this SPRs analysis concludes that PECH(SO_2)-T reveals much better selectivity than PECH(S)-T for sensing the Hg^{2+} ion from the other metal ions.

The differences between the water sorption and Hg^{2+} ion sensing behaviors of PECH(S)-T and PECH(SO_2)-T are due to the differences between their morphological structures. As discussed above, the PECH(S)-T films are amorphous, and thus, the PECH(S)-T molecules are highly mobile. Water molecules were found to induce multi-bilayer structure formation in the film, which indicates that the brush polymer has good affinity with water molecules. The polymer is composed of a hydrophilic polyoxyethylene backbone as well as hydrophilic sulfur linkers and thymine end groups in the bristles, in addition to the hydrophobic alkyl linkers. Thus, the observed high water swelling of PECH(S)-T is due to the contributions of its amorphous characteristics and hydrophilic chemical components. Nevertheless, PECH(S)-T exhibits reasonably fair performance (i.e., reasonably fair sensitivity, selectivity, and reversibility) in sensing Hg^{2+} ions. This mercury sensing performance is likely to be due to the amorphous characteristics of the polymer film, which has a relatively low population of thymine moieties on its surface. In contrast, PECH(SO_2)-T molecules tend to self-assemble in films, resulting in the formation of a molecular multi-bilayer structure that provides a thymine-rich surface. This multi-bilayer structure was found to be stable dimensionally in ambient air and even in water and metal ion solutions. PECH(SO_2)-T was found

to be more hydrophilic than PECH(S)-T. Despite its hydrophilic characteristics, the films of PECH(SO_2)-T undergo much less water swelling than the PECH(S)-T films. However, PECH(SO_2)-T films demonstrate surprisingly excellent performance (i.e., superior sensitivity, selectivity, and reversibility) in sensing Hg^{2+} ions. Thus, the observed low water swelling behavior is attributed to the stable multi-bilayer structure, which suppresses water diffusion in the PECH(SO_2)-T films. The superior performance of PECH(SO_2)-T in mercury sensing is due to the thymine-rich surface, which is stable because of the multi-bilayer structure formed in the PECH(SO_2)-T film.

The above results indicate that a thymine-rich surface is necessary for recyclable thymine-based polymers to exhibit superior sensitivity, selectivity, and reversibility in the sensing of mercury ions. This study has demonstrated that thymine-rich surfaces can be achieved by using a brush polymer bearing thymine moieties at the bristle ends that is able to self-assemble into a multi-bilayer structure.

4. CONCLUSIONS

In this study, we successfully synthesized new brush polyoxyethylenes bearing thymine moieties at the bristle ends: PECH(S)-T and PECH(SO_2)-T. They are thermally stable up to 225 °C and exhibit glass transitions in the range 23−27 °C. Despite the similarity of their chemical structures, PECH(SO_2)-T films are more hydrophilic but adsorb less water than PECH(S)-T films. Moreover, PECH(SO_2)-T films respond to mercury ions much more sensitively and selectively than PECH(S)-T films, and their binding reaction with mercury ions is fully reversible, unlike that of PECH(S)-T films.

These interesting differences are attributed to the differences between the morphological structures of the brush polymers in films. The PECH(SO_2)-T film forms a multi-bilayer structure without interdigitation, in which the layers stack along the out-of-plane region of the film, providing a thymine-rich surface. In contrast, the PECH(S)-T film is amorphous with a relatively low population of thymine moieties at the surface. The formation of the multi-bilayer structure in the PECH(SO_2)-T film is attributed to the dipole−dipole interactions between the sulfone linkers in the bristles and the hydrogen-bonding interactions between the thymine end groups. The multi-bilayer structure in the film is retained in water and even in metal ion solutions. In the case of PECH(S)-T films, the formation of a multi-bilayer structure can be induced by association with water and metal ions.

In conclusion, this study has demonstrated that a thymine-rich surface is necessary for recyclable thymine-based polymers to exhibit superior sensitivity, selectivity, and reversibility in the sensing of mercury ions. Such thymine-rich surfaces can be achieved by using a brush polymer bearing thymine moieties at the bristle ends that is able to self-assemble into a multi-bilayer structure.

■ ASSOCIATED CONTENT

Supporting Information. ^{1}H NMR spectra of the brush polymers measured in DMSO-d_6; TGA and DSC thermograms of the brush polymers, which were measured at a heating rate of 10.0 °C/min under a nitrogen atmosphere; and the out-of-plane, azimuthal angle, and in-plane scattering profiles extracted from the 2D GIXS patterns of PECH(S)-T and PECH(SO_2)-T films. This material is available free of charge via the Internet at http://pubs.acs.org.

■ AUTHOR INFORMATION

Corresponding Author

*(H.K.) Tel: +82-54-770-2417. Fax: +82-54-749-5538. E-mail: hskim@dongguk.ac.kr. (M.R.) Tel: +82-54-279-2120. Fax: +82-54-279-3399. E-mail: ree@postech.edu.

Author Contributions

J.J., J.C.K., and Y.R. contributed equally to this work.

■ ACKNOWLEDGMENT

This study was supported by the National Research Foundation (NRF) of Korea (Basic Research Grant No. 2010-0023396 and Center for Electro-Photo Behaviors in Advanced Molecular Systems (2010-0001784)) and the Ministry of Education, Science and Technology (MEST) (Korea Brian 21 Program and World Class University Program (R31-2008-000-10059-0)). The synchrotron X-ray scattering measurements at the Pohang Accelerator Laboratory were supported by MEST and POSCO Company, and POSTECH Foundation.

■ REFERENCES

(1) (a) Basu, N.; Kwan, M.; Chan, H. M. *J. Toxicol. Environ. Health Part A* **2006**, *69*, 1133–1143. (b) Grandjean, P.; Heihe, P.; White, R. F.; Debes, F. *Environ. Res.* **1998**, *77*, 165–172.

(2) (a) Chae., M. Y.; Czarnik, A. W. *J. Am. Chem. Soc.* **1992**, *114*, 9704–9705. (b) Yoon, J.; Ohler, N. E.; Vance, D. H.; Aumiller, W. D.; Czarnik, A. W. *Tetrahedron Lett.* **1997**, *38*, 3845–3848. (c) Winkler, J. D.; Bowen, C. M.; Michelet, V. *J. Am. Chem. Soc.* **1998**, *120*, 3237–3242. (d) Hennrich, G.; Sonnenschein, H.; Resch-Genger, U. *J. Am. Chem. Soc.* **1999**, *121*, 5073–5074. (e) Zhang, X. B.; Guo, C. C.; Li, Z. Z.; Shen, G. L.; Yu, R. Q. *Anal. Chem.* **2002**, *74*, 821–825.

(3) (a) Descalzo, A. B.; Martinez-Manez, R.; Radeglia, R.; Rurack, K.; Soto, J. *J. Am. Chem. Soc.* **2003**, *125*, 3418–3419. (b) Nolan, E. M.; Lippard, S. J. *J. Am. Chem. Soc.* **2003**, *125*, 14270–14271. (c) Caballero, A.; Martínez, R.; Lloveras, V.; Ratera, I.; Vidal-Gancedo, J.; Wurst, K.; Tárraga, A.; Molina, P.; Veciana, J. *J. Am. Chem. Soc.* **2005**, *127*, 15666–15667. (d) Lin, C.-Y.; Yu, C.-J.; Lin, Y.-H.; Tseng, W.-L. *Anal. Chem.* **2010**, *82*, 6830–6837.

(4) (a) Berg, C. M. G. V. D. *J. Electroanal. Chem.* **1986**, *215*, 111–121. (b) Widmann, A.; Berg, C. M. G. V. D. *Electroanalysis* **2005**, *17*, 825–831.

(5) (a) Chah, S.; Yi, J.; Zare, R. N. *Sens. Actuators, B* **2004**, *99*, 214–222. (b) Forzani, F. S.; Zhang, H.; Chen, W.; Tao, N. *Environ. Sci. Technol.* **2005**, *39*, 1257–1262.

(6) Díez-Gil, C.; Martínez, R.; Ratera, I.; Hirsh, T.; Espinosa, A.; Tárraga, A.; Molina, P.; Wolfbeis, O. S.; Veciana, J. *Chem. Commun.* **2011**, *47*, 1842–1844.

(7) (a) Tanaka, Y.; Oda, S.; Yamaguchi, H.; Kondo, Y.; Kojima, C.; Ono, A. *J. Am. Chem. Soc.* **2006**, *129*, 244–255. (b) Miyake, Y.; Togashi, H.; Tashiro, M.; Yamaguchi, H.; Oda, S.; Kudo, M.; Tanaka, Y.; Kondo, Y.; Sawa, R.; Fujimoto, T.; Machinami, T.; Ono, A. *J. Am. Chem. Soc.* **2006**, *128*, 2172–2173.

(8) (a) Ono, A.; Togashi, H. *Angew. Chem., Int. Ed.* **2004**, *43*, 4300–4302. (b) Liu, X.; Tang, Y.; Wagn, L; Zhang, J.; Song, S.; Fan, C.; Wang, S. *Adv. Mater.* **2007**, *19*, 1471–1474. (c) Liu, C.-W.; Huang, C.-C.; Chang, H.-T. *Langmuir* **2008**, *24*, 8346–8350. (d) Ren, X.; Xu, Q.-H. *Langmuir* **2009**, *25*, 29–31. (e) Liu, S.-J.; Nie, H.-G.; Jiang, J.-H.; Shen, G.-L.; Yu, R.-Q. *Anal. Chem.* **2009**, *81*, 5724–5730. (f) Wu, D.; Zhang, Q.; Chu, X.; Wang, H.; Shen, G.; yu, R. *Biosens. Bioelectron.* **2010**, *26*, 1025–1031. (g) Xue, X.; Wang, F.; Liu, X. *J. Am. Chem. Soc.* **2008**, *130*, 3244–3245. (h) Darbha, G. K.; Singh, A. K.; Rai, U. S.; Yu,

Y. H.; Ray, P. C. *J. Am. Chem. Soc.* **2008**, *130*, 8038–8043. (i) Dave, N.; Chan, M. Y.; Huang, P.-J. J.; Smith, B. D.; Liu, J. *J. Am. Chem. Soc.* **2010**, *132*, 12668–12673.

(9) (a) Tang, Y.; He, F.; Yu, M.; Feng, F.; An, L.; Sun, H.; Wang, S.; Li, Y.; Zhu, D. *Macromol. Rapid Commun.* **2006**, *27*, 389–392. (b) Lv, J.; Ouyang, C.; Yin, X.; Zheng, H.; Zuo, Z.; Xu, J.; Liu, H.; Li, Y. *Macromol. Rapid Commun.* **2008**, *29*, 1588–1592.

(10) (a) Yoon, J.; Kim, K. W.; Kim, J.; Heo, K.; Jin, K.; Jin, S.; Shin, T. J.; Lee, B.; Rho, Y.; Ahn, B.; Ree, M. *Macromol. Res.* **2008**, *16*, 575–585. (b) Bolze, J.; Kim, J.; Lee, B.; Shin, T. J.; Huan, J. Y.; Rah, S.; Youn, H. S.; Ree, M. *Macromol. Res.* **2002**, *10*, 2–2. (c) Lee, B.; Park, Y.-H.; Hwang, Y.; Oh, W.; Yoon, J.; Ree, M. *Nat. Mater.* **2005**, *4*, 147–150. (d) Lee, B.; Oh, W.; Hwang, Y.; Park, Y.-H.; Yoon, J.; Jin, K. S.; Heo, K.; Kim, J.; Kim, K.-W.; Ree, M. *Adv. Mater.* **2005**, *17*, 696–701. (e) Lee, B.; Yoon, J.; Oh, W.; Hwang, Y.; Heo, K.; Jin, K. S.; Kim, J.; Kim, K.-W.; Ree, M. *Macromolecules* **2005**, *39*, 3395–3405. (f) Lee, B.; Oh, W.; Yoon, J.; Hwang, Y.; Kim, J.; Landes, B. G.; Quintana, J. P.; Ree, M. *Macromolecules* **2005**, *38*, 8991–8995.

(11) (a) Heo, K.; Jin, K. S.; Yoon, J.; Jin, S.; Oh, W.; Ree, M. *J. Phys. Chem. B* **2006**, *110*, 15887–15895. (b) Heo, K.; Oh, K. S.; Yoon, J.; Jin, K. S.; Jin, S.; Choi, C. K.; Ree, M. *J. Appl. Cryst.* **2007**, *40*, s614–s619. (c) Jin, K. S.; Heo, K.; Oh, W.; Yoon, J.; Lee, B.; Hwang, Y.; Kim, J.-S.; Park, Y.-H.; Chang, T.; Ree, M. *J. Appl. Crystllogr.* **2007**, *40*, s631–s636. (d) Heo, K.; Park, S. G.; Yoon, J.; Jin, K. S.; Jin, S.; Rhee, S. W.; Ree, M. *J. Phys. Chem. C* **2007**, *111*, 10848–10854.

(12) Chah, S.; Yi, J.; Zare, R. N. *Sens. Actuators, B* **2004**, *99*, 214–222.

(13) (a) Callau, L.; Reina, J. A.; Mantecon, A.; Tessier, M.; Spassky, N. *Macromolecules* **1999**, *32*, 7790–7797. (b) Kim, G.; Park, S.; Jung, J.; Heo, K.; Yoon, J.; Kim, H.; Kim, I. J.; Kim, J. R.; Lee, J. I.; Ree, M. *Adv. Funct. Mater.* **2009**, *19*, 1–14.

(14) Lee, G.−C; Litt, M.H; Rogers, C. E. *Macromolecules* **1997**, *30*, 3766–3774.